

Fracture strength of glass analysed by different testing procedures

A. R. Migliore Jnr & E. D. Zanotto¹

Federal University of São Carlos, Department of Materials Engineering,
São Carlos - SP 13565-905, Brazil

Manuscript received 12 December 1995
Accepted 15 January 1996

Theoretical relations between the fracture strength of glass specimens subjected to different testing procedures are reviewed. The following techniques are analysed: pure bending, three and four point bending and the Brazilian disk test. A full derivation is presented for the Brazilian disk test. The relative severity of each testing technique is discussed.

The fracture strength of glasses and brittle materials in general depend on the size, spatial distribution and geometry of micro-defects on the specimen surface (or in the volume), as well as on the probability of these defects being subjected to a critical stress. The fracture probability, F , of brittle materials under stress is often described by the Weibull statistics⁽¹⁾

$$F = 1 - \exp(-B) \quad (1)$$

where B is a function of the defect distribution and is denominated as the Weibull integral.

Glasses and ceramics, submitted to simple tension tests, are particularly sensitive to random parasitic bending moments and the fracture stress results are often masked, as discussed by Marschall & Rudnick.⁽²⁾ Thus, other procedures are normally employed to estimate the maximum stress, (σ_{\max}) supported by a given specimen. The most common are the three and four point bending tests. Another technique used to evaluate the fracture stress is the diametral compression test of disks and cylinders (the Brazilian test). Pure bending tests are only applied to fibre specimens.

Although the solutions presented here are available in the literature, they are scattered in several papers and books, and each author uses his own notation making it difficult to find out the relevant equations needed to compare fracture results obtained in different tests. In this communication we intend to put together all relevant equations using a common notation. Particular emphasis, including a full derivation, will be given to the Brazilian disk test because, in spite of its experimental simplicity and ease of sample preparation,⁽³⁾ it has not been frequently explored to study glass fracture behaviour. Finally, a comparison of the relative severity of each test will be made.

¹ Author to whom correspondence should be addressed
E-mail: dedz@power.ufscar.br

The effect of volume on glass strength

In its simplest form, the Weibull integral for a specimen of volume V , subjected to a stress σ ($\sigma > 0$ refers to tensile stress), can be expressed as

$$B = \begin{cases} \int \left(\frac{\sigma}{\sigma_0} \right)^m dV & \text{for } \sigma > 0 \quad (2a) \\ 0 & \text{for } \sigma \leq 0 \quad (2b) \end{cases}$$

where m and σ_0 are material properties. The first is a dimensionless parameter and the second has dimensions of $[\text{stress}] \times [\text{volume}]^{1/m}$.

For the case of pure tensile testing, the stresses in any section normal to the direction of the applied force, are given by $\sigma = \sigma_{\max}$. Thus, Equation (2a) becomes

$$B = \left(\frac{\sigma_{\max}}{\sigma_0} \right)^m V \quad (3)$$

When the specimen is subjected to a variable stress state, Equation (2a) must be evaluated by performing the integral over all volume elements, dV . Hence for any stress state, Equation (3) can be rewritten as

$$B = \left(\frac{\sigma_{\max}}{\sigma_0} \right)^m \left\{ V \left(\frac{V_e}{V} \right) \right\} \quad (4)$$

where V_e is the effective volume. V_e can be defined as the theoretical volume of a sample under uniform stress, σ_{\max} having identical fracture probability of a sample with volume V subjected to a nonuniform stress state, with identical fracture stress σ_{\max} . Hence, two specimens with effective volumes V_{e1} and V_{e2} have identical fracture probability when subjected to stresses σ_1 and σ_2 , which satisfy the following relation

$$\sigma_1^m V_{e1} = \sigma_2^m V_{e2} \quad (5)$$

This relation explains the well known fact that the larger the specimen size the smaller its fracture strength.

Bending tests

Figure 1 shows a schematic load, P , on a prismatic specimen, in a typical bending test. The inner load positions are defined by a dimensionless parameter, β . In

the case of four point bending, for which the internal loads are symmetrically applied at 1/4 of the distance L , $\beta=1/4$. The normal stress σ_x , parallel to the specimen axis, can be calculated for any volume element, using the elementary beam theory.⁽⁴⁾

Specimens of rectangular cross section

For specimens having rectangular cross sections, of width, b and height, h ⁽⁴⁾

$$\sigma_{\max} = 3\beta PL/bh^2 \tag{6}$$

and thus integration of Equation (2a) leads to

$$B = \left(\frac{\sigma_{\max}}{\sigma_0} \right)^m \left(\frac{m(1-2\beta)+1}{2(m+1)^2} \right) V \tag{7}$$

where the term in the second parenthesis is the effective volume V_e . Thus, $\lambda = V_e/V$ is a dimensionless parameter, known as the normalised effective volume, which depends only on the Weibull constant, m and on the stress distribution. Thus, it does not depend on the absolute stress values. Davies⁽⁵⁾ gives an algebraic solution that coincides with Equation (7).

In the case of three-point bending ($\beta=1/2$) one has

$$\lambda = \frac{1}{2(m+1)^2} \tag{8}$$

whereas for the case of four point bending with $\beta=1/4$

$$\lambda = \frac{m+2}{4(m+1)^2} \tag{9}$$

Kittl⁽⁶⁾ studied the case of pure bending where the specimen (normally in the form of a fibre) is subjected to a constant moment, M , over a distance L . Equation (7) can be adapted to include this situation by making $\beta=0$ and using

$$\sigma_{\max} = 6M/bh^2 \tag{10}$$

Thus, in the case of pure bending, the normalised volume is

$$\lambda = \frac{1}{2(m+1)} \tag{11}$$

Specimens of circular cross section

For specimens having circular cross sections of diameter D , one has

$$\sigma_{\max} = 16\beta PL/\pi D^3 \tag{12}$$

In the case of three point bending, the normalised vol-

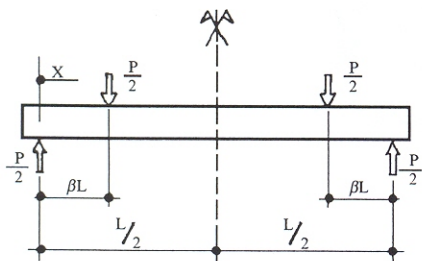


Figure 1. Schematic load position in a bending test

ume is

$$\lambda = \frac{1}{2\sqrt{\pi}(m+1)} \frac{\Gamma\left(\frac{m+1}{2}\right)}{\Gamma\left(\frac{m+4}{2}\right)} \tag{13}$$

where Γ is the gamma function. In the case of four point bending, with $\beta=1/4$

$$\lambda = \frac{1}{2\sqrt{\pi}(m+1)} \frac{\Gamma\left(\frac{m+1}{2}\right)}{\Gamma\left(\frac{m+2}{2}\right)} \tag{14}$$

For pure bending ($\beta=0$)

$$\lambda = \frac{1}{2\sqrt{\pi}} \frac{\Gamma\left(\frac{m+1}{2}\right)}{\Gamma\left(\frac{m+4}{2}\right)} \tag{15}$$

Kittl⁽⁶⁾ gives algebraic solutions which agree with Equations (13) and (15). Medrano & Gillis⁽⁸⁾ give a numerical solution which agrees with Equation (15).

The Brazilian disk test

Figure 2 schematically shows the geometrical characteristics of the diametral compression test of cylinders or disks of thickness, t where the load, P is applied in a strip of finite width, defined by an angle α . The stresses at any coordinate point (r, θ) can be obtained by the Hondros equations⁽⁹⁾

$$\sigma_r = \frac{-2P}{\alpha\pi Dt} \left\{ \alpha + \sum_{n=1}^{\infty} \left[1 - \left(1 - \frac{1}{n}\right) \left(\frac{r}{D/2}\right)^2 \right] \left(\frac{r}{D/2}\right)^{2n-2} \gamma \right\} \tag{16}$$

$$\sigma_\theta = \frac{-2P}{\alpha\pi Dt} \left\{ \alpha - \sum_{n=1}^{\infty} \left[1 - \left(1 + \frac{1}{n}\right) \left(\frac{r}{D/2}\right)^2 \right] \left(\frac{r}{D/2}\right)^{2n-2} \gamma \right\} \tag{17}$$

$$\tau_{r\theta} = \frac{2P}{\alpha\pi Dt} \left\{ \sum_{n=1}^{\infty} \left[1 - \left(\frac{r}{D/2}\right)^2 \right] \left(\frac{r}{D/2}\right)^{2n-2} \gamma \right\} \tag{18}$$

where $\gamma = \sin 2n\alpha \cdot \cos 2n\theta$.

The direction of the maximum normal stress is perpendicular to direction of the applied load and is located at the circle centre. That stress is given by

$$\sigma_{\max} = \left[\frac{2P}{\pi Dt} \right] \left(\frac{\sin 2\alpha}{\alpha} - 1 \right) \tag{19}$$

The three stresses of Equations (16–18) have similar magnitude and cannot be neglected. Therefore, the

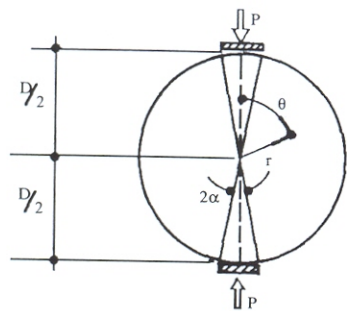


Figure 2. Schematic load position in the Brazilian test

stress state is multi-axial and is considered here with the criterion of Vardar *et al*⁽¹⁰⁾ to evaluate the effect of the normal stresses, $\sigma_n > 0$, in all planes crossed by a particular point in the sample. In this case, the Weibull integral becomes

$$B = \left(\frac{\sigma_{max}}{\sigma_0} \right)^m \int_V \eta \left[\int_A \left(\frac{\sigma_n}{\sigma_{max}} \right)^m dA \right] dV \quad (20)$$

where $dA = \sin \psi d\psi d\phi$ is the surface element of a sphere of unit radius around any point in which the principal stresses are $\sigma_1 \geq \sigma_2 \geq \sigma_3$.

The stress σ_n can be evaluated by the Batdorf & Heinisch⁽¹¹⁾ expression

$$\sigma_n = \sigma_3 + (\sigma_1 - \sigma_3) \cos^2 \psi + (\sigma_2 - \sigma_3) \cos^2 \phi \sin^2 \psi \quad (21)$$

The constant η is a correction factor of the integral in Equation (20) to satisfy the situation, in a simple tension test, where

$$\sigma_1 = \sigma_{max} \text{ and } \sigma_2 = \sigma_3 = 0 \quad (22)$$

By substituting Equations (21) and (22) into Equation (20) and integrating on the surface of the unit sphere we have

$$B = \left(\frac{\sigma_{max}}{\sigma_0} \right)^m V \eta \int_0^\pi \int_0^{2\pi} \cos^{2m} \psi \sin \psi d\phi d\psi \quad (23)$$

or

$$B = \left(\frac{\sigma_{max}}{\sigma_0} \right)^m V \eta \frac{4\pi}{2m+1} \quad (24)$$

For Equation (24) to coincide with Equation (3) it is necessary that

$$\eta = \frac{2m+1}{4\pi} \quad (25)$$

In the particular case of the Brazilian Test, Equation (20) becomes

$$B = \left(\frac{\sigma_{max}}{\sigma_0} \right)^m 4\ell \int_0^{\pi/2} \int_0^{\pi/2} \left(8\eta \int_0^{\phi_1} \int_0^{\phi_1} \left(\frac{\sigma_n}{\sigma_{max}} \right) \sin \psi d\phi d\psi \right) r dr d\theta \quad (26)$$

where ϕ_1 is the integration limit for a given angle ψ , for which $\sigma_n > 0$. It can be calculated by

$$\phi_1 = \arccos(\delta) \quad (27)$$

with

$$\delta^2 = \frac{\sigma_3 + (\sigma_1 - \sigma_3) \cos^2 \psi}{(\sigma_3 - \sigma_2) \sin^2 \psi} \quad (28)$$

For $\delta^2 \leq 0$ a plane exists where $\sigma_n > 0$ and then $\phi_1 = \pi/2$. For $\delta^2 \geq 1$ no plane exists where $\sigma_n > 0$ and then $\phi_1 = 0$.

Making $\xi = (2r/D)$ and inserting into Equation (26) gives

$$B = \left(\frac{\sigma_{max}}{\sigma_0} \right)^m \left[\frac{8V}{\pi} \int_0^{\pi/2} \int_0^{\pi/2} \left(8\eta \int_0^{\phi_1} \int_0^{\phi_1} \left(\frac{\sigma_n}{\sigma_{max}} \right) \sin \psi d\phi d\psi \right) r dr d\theta \right] \quad (29)$$

where the term into the second parenthesis is the effective volume. Equation (29) was integrated numerically in this paper. The results coincide with those of Vardar & Finnie.⁽¹²⁾ Similar results are obtained if the specimens surfaces are considered instead of volumes.

Discussion

Figure 3 shows the variation of the normalised effective volume, $(V_e/V)^{1/m}$, with the Weibull parameter, m , for the cases of Brazilian test, pure bending, three and four point bending of specimens having rectangular and circular cross sections. As the effective volume values slightly change with load angle for the Brazilian test (V_e/V typically decreases about 3% for each 2° increment in α), only the results for $\alpha=8^\circ$ are presented.

Equation (5) shows that the fracture stress is inversely proportional to $V_e^{1/m}$. Thus, pure tensile testing ($\lambda=1$) is represented by the upper horizontal limit of Figure 3. The set of curves show that pure tensile tests lead to the smallest fracture stresses, followed by pure bending, the Brazilian test, four point bending and three point bending, in that order, for specimens of

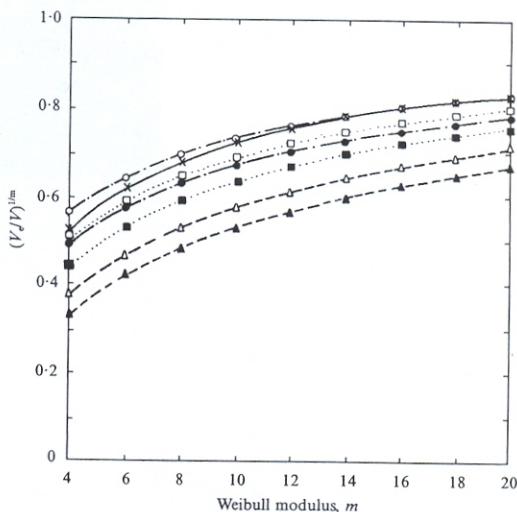


Figure 3. Variation of reduced effective volume $(V_e/V)^{1/m}$ with Weibull parameter for different testing techniques

- x— Brazilian test, $\alpha=8^\circ$
- o--- Pure—rectangular
- Pure—circular
- 4 point—rectangular
- 4 point—circular
- △--- 3 point—rectangular
- ▲--- 3 point—circular

identical volume, V . This is because the normalised effective volumes decrease in that same order. It is also verified that specimens of circular cross sections have larger fracture stresses than those of rectangular cross sections, for any bending test. This trend is maintained for increasingly large values of the Weibull modulus, m . However, the larger the value of m , the more similar are the results obtained by each technique, all tending to the pure tensile test value for $m \rightarrow \infty$ (However, for real materials, m does not exceed a value of 50).

It should be pointed out that the Brazilian test frequently utilises specimens having volumes which are one order of magnitude smaller than those of bending tests. Thus, it is expected that the results of fracture stresses obtained in Brazilian tests are greater than those obtained in bending tests. Therefore, it is possible to explain the observed differences in the average fracture stresses of glasses subjected to distinct testing procedures.

An important restriction for that comparison is that the different specimens must be prepared by identical processing techniques (for instance, identical surface finishing) to maintain a constant defect distribution and, consequently, the Weibull parameters. Hence, many fracture results reported in the literature for diametral compression tests cannot be directly compared with results obtained in bending tests due to the differ-

ent degree of surface damage of the specimens. For example, it is quite common to cut cylindrical rods to obtain specimens for the Brazilian and bending tests. However, the critical surface in the first test is perpendicular to the cylindrical axis, while it is parallel to that axis in bending tests. Thus, the surface finishing and, consequently, the Weibull parameters are different. In that case, Equation (5) cannot be used. Finally, great care with the sample supports should be exercised when performing the actual mechanical testing, to minimise parasitic stresses, as demonstrated recently by Migliore & Zanotto.⁽¹³⁾

References

1. Weibull, W. *J. Appl. Mech.*, 1951, **18**, 293.
2. Marschall, W. & Rudnick, A. In *Fracture mechanics of ceramics*. Vol. 1. Plenum Press, New York. P 69.
3. Marion, R. H. & Johnstone, J. K. *Ceram. Bull.*, 1977, **56**, 998.
4. Higdon, A., Ohlsen, E. H., Stiles, W. B., Weese, J. A. & Riley, W. F. In *Mechanics of materials*, 1976. Wiley, New York. P 239.
5. Davies, G. S. In *Proc. n 22—British Ceramic Society*. 1973. Edited by D. J. Godfrey. British Ceramic Society, Stoke-on-Trent. Proceedings of the Meeting in Cambridge, July 1972. P 429.
6. Kittl, P. *Res. Mechanica*, 1980, **1**, 161.
7. Korn, G. A. & Korn, T. M. In *Mathematical handbook for scientists and engineers*. 1961. McGraw-Hill, New York. P 819.
8. Medrano, R. E. & Grills, P. P. *J. Am. Ceram. Soc.*, 1987, **70**, P C230.
9. Hondros, G. *Austr. J. Appl. Sci.*, 1974, **10**, 243.
10. Oh, K. P., Vardar, O & Finnie, I. *Int. J. Fract.*, 1973, **9**, 372.
11. Batdorf, B. & Heinisch, H. L. *Jnr J. Am. Ceram. Soc.*, 1978, **61**, 355.
12. Vardar, Ö. & Finnie, I. *Int. J. Fract.*, 1975, **11**, 495.
13. Migliore, A. R. *Jnr & Zanotto, E. D. Glass Technol.*, 1995, **36** (2) 65–6.